Water Science and Engineering, 2010, 3(3): 321-330
doi:10.3882/j.issn.1674-2370.2010.03.008

http://www.waterjournal.cn
e-mail: wse2008@vip.163.com

Orifice plate cavitation mechanism and its influencing factors

Wan-zheng AI*, Tian-ming DING

Marine College of Zhejiang Ocean University, Zhoushan 316000, P. R. China

Abstract: The orifice plate energy dissipater is an economic and highly efficient dissipater. However, there is a risk of cavitaion around the orifice plate flow. In order to provide references for engineering practice, we examined the cavitation mechanism around the orifice plate and its influencing factors by utilizing mathematical analysis methods to analyze the flow conditions around the orifice plate in view of gas bubble dynamics. Through the research presented in this paper, the following can be observed: The critical radius and the critical pressure of the gas nucleus in orifice plate flow increase with its initial state parameter τ_0 ; the development speed of bubbles stabilizes at a certain value after experiencing a peak value and a small valley value; and the orifice plate cavitation is closely related to the distribution of the gas nucleus in flow. For computing the orifice plate cavitation number, we ought to take into account the effects of pressure fluctuation. The development time of the gas nucleus from the initial radius to the critical radius is about 10^{-7}-10^{-5} s; therefore, the gas nucleus has sufficient time to develop into bubbles in the negative half-cycle of flow fluctuation. The orifice critical cavitation number is closely related to the orifice plate size, and especially closely related with the ratio of the orifice plate radius to the tunnel radius. The approximate formula for the critical cavitation number of the square orifice plate that only considers the main influencing factor was obtained by model experiments.

Key words: *orifice plate cavitation; gas nucleus; critical radius; critical pressure; pressure fluctuation; critical cavitation number*

1 Introduction

The orifice plate energy dissipater has the advantages of a simple layout, economy, and high energy efficiency (He and Zhao 2010). The energy dissipation efficiency of the orifice plate and its cavitations are a pair of contradictions. Orifice plates with high efficiency of energy dissipation often have a high risk of cavitation damage. Cavitation can lead to structural damage of buildings and reduce spillway tunnel discharge capacity (Rahmeyer 1988; Plesst and Zwick 1977; Zhang and Chai 2001; Neppiras 1984). Cavitation can be divided into four categories: wavering cavitation, fixed cavitation, vortex cavitation, and oscillation cavitation (Knapp et al. 1970). Oscillation cavitation and vortex cavitation are the main forms of orifice plate cavitation (Xu et al. 1988). The study of cavitation has been mainly focused on model tests in the past and some useful conclusions have been obtained. Many studies have

This work was supported by the National Natural Science Foundation of China (Grant No. 50879021).
*Corresponding author (e-mail: *aiwanzheng@126.com*)
Received Nov. 22, 2008; accepted Feb. 27, 2009

concluded that the orifice plate critical cavitation number decreases with the increase of the contraction ratio (Xu et al. 1988; Russell and Ball 1967). The successful application of the orifice plate energy dissipater in the Xiaolangdi Project in China has proved that installing orifice plates in tunnels, as shown in Fig. 1, where D and d are the diameters of the channel and orifice plate, T and b are the thicknesses of the orifice plate and anti-vortex ring, r is the radius of the round corner of the orifice plate, β is the slope angle at the top of the orifice plate, and θ is the slope angle of the anti-vortex ring, is an effective way to dissipate flow energy (Chen et al. 2006). However, orifice plate cavitation is a very complex problem, and there has been little research on the orifice plate cavitation mechanism and its influencing factors, especially on the principle of cavitation caused by pressure fluctuation. Based on a summary of previous results, this paper attempts to further reveal the mechanism of the orifice plate cavitation and to analyze factors that affect its cavitation in view of gas bubble dynamics.

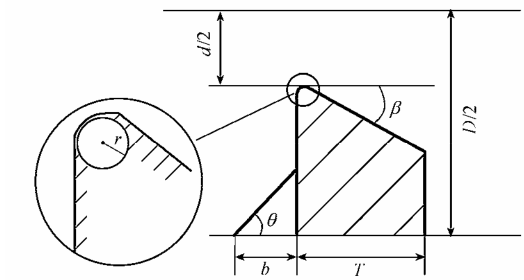

Fig. 1 Orifice plate with anti-vortex ring

2 Orifice plate cavitation mechanism

In low-pressure conditions, the motion equation of a gas nucleus developing into a gas bubble is as follows (Huang and Han 1992):

$$R\frac{\mathrm{d}U}{\mathrm{d}t}+\frac{3}{2}U^2=C_0^2\left(\frac{R_0}{R}\right)^{3\gamma}-\frac{2\sigma}{\rho R}-\frac{1}{\rho}\left(p_\infty-p_\mathrm{v}\right)=f\left(R,t\right) \tag{1}$$

where $C_0^2=p_1/\rho$; p_1 is the gas nucleus initial pressure; ρ is the flow density; U is the gas nucleus development velocity, which can be expressed as $U=\mathrm{d}R/\mathrm{d}t$; R is the radius of the gas nucleus; R_0 is the initial radius of the gas nucleus; t is time; γ is the air insulation coefficient; σ is the surface tension coefficient; p_v is the saturated steam pressure; and p_∞ is the pressure on the non-disturbed sections, usually located at 0.5D in front of the orifice plate or at 3D behind the orifice plate, shown in section 1 and section 2, respectively, in Fig. 2 (Xu et al. 1988), where L_b is the length of the backflow region behind the orifice plate. p_∞ is also affected by the orifice plate geometry.

If $\partial f/\partial R=0$, we can obtain the critical radius of the gas nucleus:

$$R_\mathrm{c}=\left(\frac{2\sigma}{3\rho C_0^2R_0^{3\gamma}\gamma}\right)^{\frac{1}{1-3\gamma}} \tag{2}$$

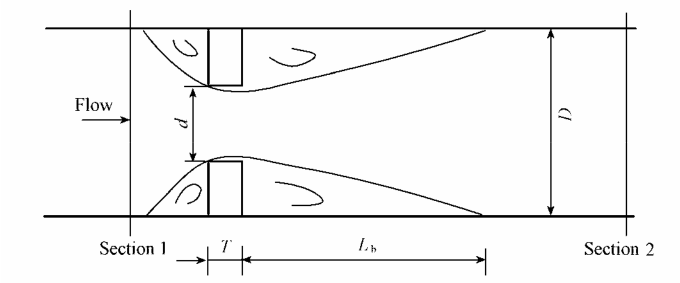

Fig. 2 Flow around orifice plate

If $R = R_c$ and $f(R,t) = 0$, we can obtain the critical pressure of the gas nucleus:

$$p_c = \frac{2\sigma(1-3\gamma)}{3R_c\gamma} + p_v \tag{3}$$

If $\tau_0 = p_1 R_0^{3\gamma}$ (τ_0 represents the initial state parameters of the gas nucleus), we can obtain the following equations:

$$R_c = \left(\frac{2\sigma}{3\tau_0\gamma}\right)^{\frac{1}{1-3\gamma}} \tag{4}$$

$$p_c = \frac{2\sigma(1-3\gamma)}{3\gamma\left[2\sigma/(3\tau_0\gamma)\right]^{\frac{1}{1-3\gamma}}} + p_v \tag{5}$$

Figs. 3 and 4 can be obtained at the normal temperature when $\gamma = 4/3$, $\sigma \approx 0.072\ 8\ \text{N/m}$, and $p_v \approx 2\ 452\ \text{Pa}$, and the following can be observed: R_c and p_c increase with τ_0, that is to say, R_c and p_c increase with p_1 and R_0; and if $\tau_0 \to \infty$, $p_c \to p_v$. Therefore, many researchers regard p_v as the critical pressure of incipient cavitation. In fact, if τ_0 is large enough, there is a little deviation between p_v and p_c, but if τ_0 is small, there is a large deviation between p_v and p_c, and it is not accurate to regard p_v as the critical pressure of incipient cavitation under this condition. Integrating Eq. (1), the following equation can be given:

$$U = \frac{\mathrm{d}R}{\mathrm{d}t} = \left\{\frac{2C_0^2}{3(1-\gamma)}\left[\left(\frac{R_0}{R}\right)^{3\gamma} - \left(\frac{R_0}{R}\right)^3\right] + \frac{2\sigma}{\rho R}\left[\left(\frac{R_0}{R}\right)^2 - 1\right] + \frac{2}{3}\frac{(p_\infty - p_v)}{\rho}\left[\left(\frac{R_0}{R}\right)^3 - 1\right]\right\}^{\frac{1}{2}} \tag{6}$$

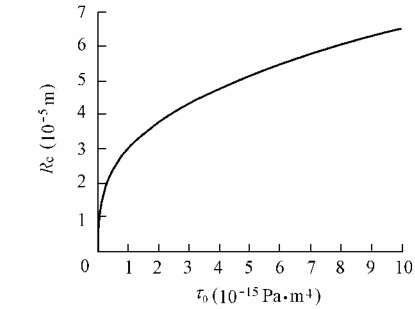

Fig. 3 R_c-τ_0 curve

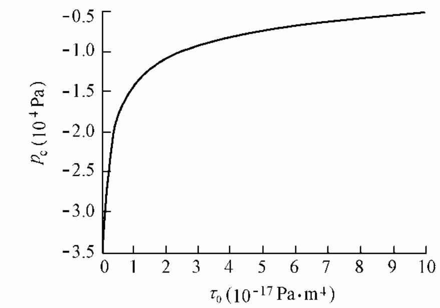

Fig. 4 p_c-τ_0 curve

The simulation results of Eq. (6) are shown in Fig. 5, which reflect the relationship between U and R at the normal temperature when $p_\infty = 600\ \text{Pa}$, and $p_1 = 4\ 500\ \text{Pa}$ or $3\ 500\ \text{Pa}$.

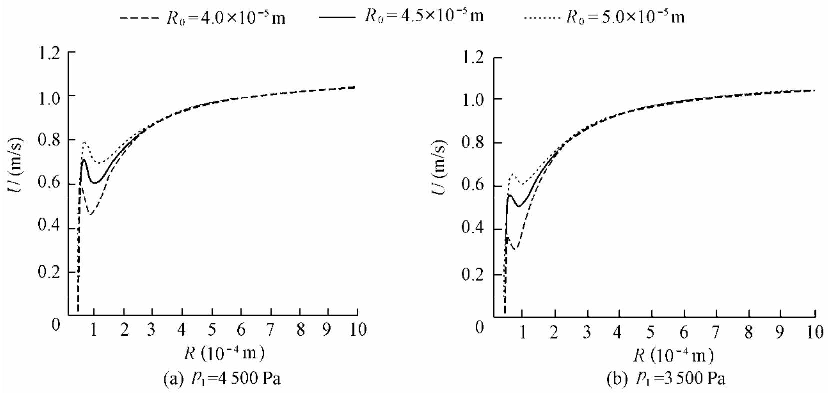

Fig. 5 U-R curve

Fig. 5 shows that, in the initial phase, the development velocity of the gas nucleus increases with its radius. When the gas nucleus radius develops into the critical radius, the development velocity of the gas nucleus has a small peak value. At this time, cavitation begins to occur. The critical radii of the gas nucleus, when $p_1 = 4\ 500\ \text{Pa}$, are 9.18×10^{-5} m, 7.97×10^{-5} m, and 6.82×10^{-5} m, respectively corresponding to initial radii of 5×10^{-5} m, 4.5×10^{-5} m, and 4×10^{-5} m; and the critical radii of the gas nucleus, when $p_1 = 3\ 500\ \text{Pa}$, are 8.44×10^{-5} m, 7.23×10^{-5} m, and 6.27×10^{-5}m, respectively corresponding to initial radii of 5×10^{-5} m, 4.5×10^{-5}m, and 4×10^{-5}m. If the gas nucleus inflation continues, the development velocity of the gas nucleus reaches a small valley value. After that, the development velocity of the gas nucleus increases with the radius and at last stabilizes at a certain value. For the gas nucleus with the same initial radius, if the initial pressure of the gas nucleus is larger, its inflation velocity at a critical radius is also larger. For the gas nucleus with the same initial pressure, if the initial radius of the gas nucleus is larger, its inflation velocity at a critical radius is also larger. If $F\left(R, p_\infty - p_\text{v}\right) = U$, we obtain the development time of the gas nucleus from the initial radius to the critical radius:

$$\Delta t = \int_{R_0}^{R_\text{c}} \frac{\mathrm{d}R}{F\left(R, p_\text{c} - p_\text{v}\right)} \tag{7}$$

The range of the initial radius of the gas nucleus is 2×10^{-6} m to 50×10^{-6} m in normal flow (Ni 1999). At this range, if gas nuclei can develop into gas bubbles, the following conditions must be met: $p_\infty \le p_\text{c}$ and $p_1 > p_\infty - p_\text{v} + 2\sigma/R_0$. Table 1 shows the development time of the gas nucleus under the conditions of $\sigma \approx 0.072\ 8\ \text{N/m}$, $p_\text{v} \approx 2\ 452\ \text{Pa}$, $\gamma = 4/3$, and R_0 ranging from 0.05×10^{-6} m to 50×10^{-6} m.

Table 1 Development time of gas nucleus from initial radius to critical radius for different initial parameters

R_0 (10^{-5} m)	p_1 (Pa)	R_c (10^{-5} m)	p_c (Pa)	p_λ (Pa)	p_∞ (Pa)	Development state	Δt (10^{-5} s)
4.50	4 500.00	7.97	1 082.61	3 716.44	500.00	Development	4.36
4.00	4 500.00	6.82	849.75	3 312.00	600.00	Development	4.13
1.00	4 500.00	1.07	−7 721.47	−7 608.00	1 000.00	No development	
4.00	3 500.00	6.27	709.75	2 312.00	600.00	Development	4.38
0.10	156 350.00	0.18	−59 590.00	143 000.00	−59 590.00	Development	0.03
4.50	4 500.00	7.97	1 082.62	3 716.44	400.00	Development	4.22
4.50	4 500.00	7.97	1 082.61	3 716.44	600.00	Development	4.51

Note: $p_\lambda = p_\infty - p_v + 2\sigma/R_0$.

From Table 1 we can observe the following: The development time of the gas nucleus from the initial radius to the critical radius is about 10^{-7}-10^{-5} s. Under the condition of the same p_∞ and R_0, the gas nucleus with a larger p_1 will need less time to develop into the critical radius. Under the condition of the same p_1 and R_0, the gas nucleus with a larger p_∞ will need a longer time to develop into the critical radius. Under the condition of the same p_1 and p_∞, the gas nucleus with a larger R_0 will need a longer time to develop into the critical radius.

Physical factors that affect the gas nucleus development include R_0, p_1, and p_∞. R_0 and p_1 determine the initial state parameter τ_0, that is to say, if R_0 and p_1 are determined, p_c and R_c are also determined. If R_0, p_1, and p_∞ are determined, the development time of the gas nucleus from the initial radius to the critical radius is also determined.

Two conditions determine whether cavitations happen in orifice plate flow or not. One is whether there are many gas nuclei and whether gas nuclei meet this condition: $p_1 = p_{out} - p_v + 2\sigma/R_0$, where p_{out} is the pressure outside the gas nucleus. That is to say, the orifice plate cavitation is closely related with the distribution of gas nuclei in flow. The other is whether there is a low pressure condition for gas nucleus development, i.e., $p_\infty \le p_c$ and $p_1 > p_\infty - p_v + 2\sigma/R_0$. When flow passes through the orifice plate, streamlines suddenly shrink, and then suddenly enlarge, which causes boundary layer separation. Therefore, the boundary layer is closely related with cavitation. Meanwhile, whirlpool areas occur in front of and behind the orifice plate. At the center of a whirlpool area, there often form low pressure areas. At a distance about 0.5D behind the orifice plate, there is a contraction section. At fringes of the contraction section, there also form low pressure areas. In addition, because of turbulent shear, local low pressure also exists in the orifice plate flow. All these low pressure areas create favorable conditions for gas nucleus development. Thus, the orifice plate size, especially the ratio of the orifice plate radius to the tunnel radius, is closely related with the orifice plate cavitation.

3 Factors affecting orifice plate critical cavitation number

The formula for the critical cavitation number of the orifice plate is as follows:

$$\sigma_{\mathrm{c}}=\frac{p_{\infty}-p_{\mathrm{v}}}{0.5\rho u_0^2} \tag{8}$$

where u_0 is the average flow velocity in the tunnel. Cavitation is mainly affected by the flow velocity, viscosity, boundary conditions, and pressure. Therefore, the minimum pressure on the border can also be used to determine whether cavitation has occurred. The minimum pressure coefficient is defined as follows:

$$C_{\mathrm{p}}=\frac{p_{\min}-p_{\infty}}{0.5\rho u_0^2} \tag{9}$$

where $p_{\min}$ is the minimum pressure on the border. If cavitation occurs, the gas bubble is full of steam, and the pressure in the gas bubble is equal to saturated steam pressure p_{v}. Also, cavitation begins to occur at the position of the minimum pressure; at this time, $p_{\min}$ is equal to p_{v}, providing the following equation:

$$\sigma_{\mathrm{c}}=-C_{\mathrm{p}}=\frac{p_{\infty}-p_{\min}}{0.5\rho u_0^2}=\frac{\Delta p}{0.5\rho u_0^2} \tag{10}$$

For an orifice plate shown in Fig. 1, the main geometry parameters that determine boundary conditions are the tunnel diameter D, the orifice plate diameter d, the thickness of the orifice plate *T*, and the radius for the round corner of the orifice plate r. Besides these geometry parameters, the other hydraulic parameters that affect critical cavitation number are the dynamic viscosity parameter μ, the average flow velocity in the tunnel u_0, the deviation between the average pressure on the non-disturbed section and the minimum pressure on the boundary Δp. All the above parameters are written into a formula as follows:

$$f_1\left(D,d,\rho,\mu,u_0,\Delta p,r,T\right)=0 \tag{11}$$

According to the dimensional analysis, D, u_0, and ρ are three basic parameters of the above eight parameters. A non-dimensional equation can be obtained using the π theorem as follows:

$$f_2\left(\frac{d}{D},\frac{\mu}{\rho u_0 D},\frac{T}{D},\frac{r}{D},\frac{\Delta p}{\rho u_0^2}\right)=0 \tag{12}$$

The above equation is changed as follows:

$$\Delta p=\rho u_0^2 f_3\left(\frac{d}{D},\frac{\mu}{\rho u_0 D},\frac{T}{D},\frac{r}{D}\right) \tag{13}$$

Because $\mu/\left(\rho u_0 D\right)=1/Re$, where Re is the Reynolds number, the above equation can be written as

$$\Delta p=\rho u_0^2 f_3\left(\frac{d}{D},\frac{1}{Re},\frac{T}{D},\frac{r}{D}\right) \tag{14}$$

Combing Eq. (10) with Eq. (14), Eq. (15) can be rewritten as

$$\sigma_{\mathrm{c}}=-C_{\mathrm{p}}=\frac{1}{2}f_3\left(\frac{d}{D},\frac{1}{Re},\frac{T}{D},\frac{r}{D}\right) \tag{15}$$

In the above equation, d/D is the contraction ratio, and T/D and r/D are parameters of the orifice plate geometry. From Eq. (15), the following conclusion can be obtained: the orifice plate critical cavitation number is closely related with the orifice plate geometry, contraction ratio, and Reynolds number. With the assumption that

$$\eta = d/D \tag{16}$$

$$\xi' = f\left(T/D, r/D\right) \tag{17}$$

where ξ' is a parameter regarding the orifice plate geometry, Eq. (15) can be rewritten as

$$\sigma_{\mathrm{c}} = f_4\left(\eta, Re, \xi'\right) \tag{18}$$

Li et al. (1997) regarded η as the main factor affecting the critical cavitation number of the orifice plate. They also provided an empirical formula for the orifice plate critical cavitation number according to hydraulic model experiments:

$$\sigma_{\mathrm{c}} = a - b\exp\left(-cRe\right) \tag{19}$$

where a, b, and c are determined by the orifice plate geometry. Because the flow passing through the orifice plate is turbulent flow, the boundary layer has fully developed in most cases, and the critical cavitation number changes little with the change of the Reynolds number. At this time, the critical cavitation number can be expressed as

$$\sigma_{\mathrm{c}} = f\left(\eta, \xi'\right) \tag{20}$$

Most studies (Li et al. 1997; Takahashi et al. 2001) have regarded the critical cavitation number as varying with η by index relations. Thus, the critical cavitation number can be expressed as

$$\sigma_{\mathrm{c}} = m\eta^{n} \tag{21}$$

where m and n are determined by the orifice plate geometry parameters, excluding η. Eq. (21) shows that the larger the contraction ratio is, the smaller the orifice critical cavitation number is.

4 Pressure fluctuation effect on orifice plate cavitation

If we consider the effect of the flow fluctuation, we can obtain another equation about the cavitation number:

$$\sigma_t = \frac{p_\infty + p' - p_{\mathrm{v}}}{0.5\rho u_0^2} \tag{22}$$

where p' is the pressure fluctuation. Under the condition of low pressure, the gas nucleus must have enough time t_{c} to develop into a bubble. As the flows passing through the orifice plate have the characteristics of a large low-frequency fluctuation, the spectrum scope of the pressure fluctuation is about 0 to 5 Hz. Peak frequency, in general, is about 0 to 0.5 Hz. Thus, the time that flow fluctuation stays in the negative half-cycle of the fluctuation cycle will be longer than 10^{-2} s. From Table 1 we can observe that gas nucleus development time from the gas nucleus to the gas bubble is about 10^{-7}-10^{-5} s. Therefore, the gas nucleus has sufficient time to develop into bubbles in the negative half-cycle of the fluctuation cycle.

Characteristics of the flow fluctuation have important effects on the orifice plate cavitation. Under normal circumstances, cavitation will not occur when the cavitation number is larger than the critical cavitation number, i.e., when $\sigma_t > \sigma_{\mathrm{c}}$. However, the critical cavitation number of the orifice plate computed through Eq. (8) is often larger. For example, if the flow fluctuation is in the negative half-cycle of a fluctuation cycle, the pressure fluctuation is a negative value in Eq. (22). At this time, the actual cavitation number computed through Eq. (22) is smaller than the critical cavitation number computed through Eq. (8). Only when the flow fluctuation is in the positive half-cycle of a fluctuation cycle can we find that the cavitation number calculated with Eq. (22) is larger than the critical cavitation number calculated with Eq. (8). Thus we assume there is no cavitation in the orifice plate flow. Therefore, if we consider the fluctuation effect on cavitation, we will find that cavitation occurs locally.

Hu (1994) showed that, in flow fluctuation, the gas nucleus expands in a negative half-cycle at first and then is compressed in a positive half-cycle; compression and expansion of the gas nucleus appear alternately, which cause saturated gas in the flow to permeate into the gas nuclei through their side walls. In the turbulent shear flow, when cavitation begins, high-frequency components in the power spectrum of pressure fluctuation increase. In general, there is a predominant frequency. The fluctuation at the predominant frequency leads to the bubble oscillation. In the course of bubble rebounding, bubbles have a resonance movement because of the appearance and disappearance of compression in the bubble. In turn, resonance changes the pressure fluctuation. This phenomenon helps to produce a series of large and small fluctuations. These large and small fluctuations cannot be ignored; they will shorten the time the gas nucleus takes to develop into the gas bubble and cause cavitations to occur.

The intense flow fluctuations through the orifice plate are caused by the orifice plate's sudden enlargement and contraction and dramatic changes of streamlines. Fluctuation amplitude is closely related with orifice plate geometry and contraction ratio. Russell and Ball (1967) arrived at the following conclusions: when $d/D \leq 0.65$, the pressure fluctuation coefficient is almost unchanged around 0.5; when $0.85 \geq d/D > 0.65$, the pressure fluctuation coefficient increases with the contraction ratio of the orifice plate, with the peak pressure fluctuation coefficient reaching the value of 3 when $d/D = 0.85$; and when $d/D > 0.85$, the pressure fluctuation coefficient decreases with the increase of the contraction ratio. Taking into account the effects of pressure fluctuation, the critical cavitation number can be written as

$$\sigma_{\mathrm{c}} = -C_{\mathrm{pmin}} + K \frac{\sqrt{\overline{p'}^2}}{0.5\rho u_0^2} \tag{23}$$

where $\overline{p'}$ is the average value of pressure fluctuation, and K is a parameter closely related with the probability density and properties of the spectrum of pressure fluctuation. Yang et al. (2004) determined that if we consider 95% of pressure fluctuation as the characteristic value of cavitation occurrence, it is reasonable to assume a K value of 1.6.

5 Model experiments on critical cavitation number of square orifice plate

Model experiments were conducted in a decompression cabinet. The decompression cabinet was designed based on the principles of gravity similarity and cavitation number similarity. As presented in Tullis and Govindarajan (1973), the contraction ratio is the most important factor influencing the critical cavitation number of the orifice plate. Therefore, only the contraction ratio was considered in the model experiments. The models were designed as in Fig. 2. The orifice plate thickness T of each model was $0.01D$. The other parameters of the models were arranged as in Table 2. The critical cavitation number of the orifice plate was calculated by Eq. (8), but p_∞ was divided into two parts as in Eq. (24):

$$p_\infty = p_{\mathrm{u}} + p_{\mathrm{a}} \tag{24}$$

where p_{u} is the relative pressure in section 1, and p_{a} is the air pressure in the decompression cabinet. All experimental results are shown in Table 3. Fig. 6 can be drawn using the data in Table 3.

Table 2 Model parameters

Model number	D (m)	η	d (m)
M1	0.21	0.60	0.126 0
M2	0.21	0.70	0.147 0
M3	0.21	0.78	0.163 8
M4	0.21	0.80	0.168 0

Table 3 Experimental results

Model number	$p_{\mathrm{u}}/(\rho g)$ (m)	$p_{\mathrm{a}}/(\rho g)$ (m)	$p_{\mathrm{v}}/(\rho g)$ (m)	$u^2/(2g)$ (m)	σ_{c}
M1	0.651	0.311	0.192	0.031	22.621
M2	0.098	0.372	0.211	0.073	12.312
M3	0.711	0.310	0.211	0.073	7.963
M4	2.070	0.311	0.201	0.282	6.960

Fig. 6 shows that the critical cavitation number of the orifice plate inversely varies with the contraction ratio. An approximate formula for the critical cavitation number of the square orifice plate can be obtained:

$$\sigma_{\mathrm{c}} = 2.1\eta^{-4.6} \tag{25}$$

In Eq. (25), the effects of Reynolds number, pressure fluctuation and orifice plate thickness are not considered. This expression is valid for $T = 0.01D$, $Re > 10^5$, and η values from 0.6 to 0.8.

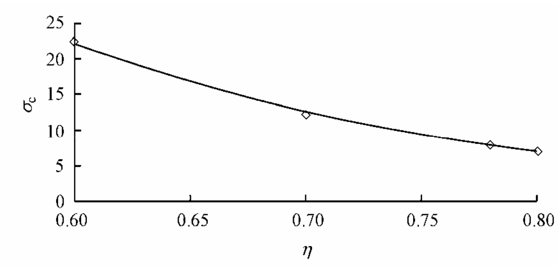

Fig. 6 σ_{c}-η curve

6 Conclusions

(1) Critical radius and critical pressure increase with the initial state parameter τ_0. That

is to say, critical radius and critical pressure increase with the gas nucleus initial radius and its initial pressure.

(2) The orifice plate cavitation is closely related with the gas nucleus distribution, the contraction ratio and geometry of the orifice plate. The larger the contraction ratio is, the smaller the critical cavitation number of the orifice plate is.

(3) The gas nucleus has sufficient time to develop into bubbles in the negative half-cycle of flow fluctuation, so the characteristics of the flow fluctuation have a certain effect on cavitation. It is necessary to take into account the effect of pressure fluctuation when computing the orifice plate cavitation number.

References

Chen, L., Wang, X. X., Wei, H., and Zhang, D. 2006. Prototype observation on cavitation for multi-orifice No. one bottom outlet Xiaolangdi Project. *Journal of Water power*, 32(2), 71-74. (in Chinese)

He, N., and Zhao, Z. X. 2010. Theoretical and numerical study of hydraulic characteristics of orifice energy dissipater. *Journal of Water Science and Engineering*, 3(2), 190-199. [doi:10.3882/j.issn.1674-2370.2010.02.007]

Hu, M. L. 1994. The influence of bubble vibration on the cavitation in turbulent shear flow. *Journal of Hydrodynamics, Ser. A*, 11(2), 182-189. (in Chinese)

Huang, J. C., and Han, C. C. 1992. Influences of gas nucleus scale on cavitations. *Applied Mathematics and Mechanics*, 13(4), 359-367. [doi:10.1007/BF02451422]

Li, Z. Y., Chen, X., and Chen, M. F. 1997. Study on hydraulic problems of spillway tunnels with orifices reformed from diversion tunnel. *Journal of Hydraulic Engineering*, 28(2), 1-14. (in Chinese)

Knapp, R. T., Daily, J. W., and Hammitt, F. G. 1970. *Cavitation*. New York: McGraw-Hill.

Neppiras, E. A. 1984. Acoustic cavitation: An introduction. *Ultrasonics*, 22(1), 25-28. [doi:10.1016/0041-624X(84)90057-X]

Ni, H. G. 1999. Correction of incipient cavitations number for scale effect. *Journal of Hydraulic Engineering*, 30(9), 28-32. (in Chinese)

Plesst, M. S., and Zwick, S. A. 1977. Bubble dynamics and cavitation. *Annual Review Fluid Mechanics*, 9, 145-185.

Rahmeyer, W. 1988. Energy dissipation and limiting discharge with orifices. *Journal of Transportation Engineering*, 114(2), 232-235. [doi:10.1061/(ASCE)0733-947X(1988)114:2(232)]

Russell, S. O., and Ball, J. W. 1967. Sudden-enlargement energy dissipater for Mica Dam. *Journal of the Hydraulic Division*, 93(4), 41-56.

Takahashi, K., Matsuda, H., and Miyamoto, H. 2001. Cavitation characteristics of restriction orifices. *CAV 2001: Fourth International Symposium on Cavitation*. Pasadena: California Institute of Technology.

Tullis, P. J., and Govindarajan, R. 1973. Cavitations and size scale effects for orifices. *Journal of the Hydraulics Division*, 99(3), 417-430.

Xu, F. S, Yu, M. X., and Liu, S. J. 1988. The characteristics of cavitation and fluctuation for multi-orifices. *Advances in Hydrodynamics*, 3(3), 68-75. (in Chinese)

Yang, Q., Zhang, J. M., Dai, G. Q., Wang, H. Y., and Cui, C. L. 2004. Effects of fluctuation pressure on cavitation. *Journal of Sichuan University (Engineering Science Edition)*, 36(4), 19-23. (in Chinese)

Zhang, Q. Y., and Chai, B. Q. 2001. Hydraulic characteristic of multistage orifice tunnels. *Journal of Hydraulic engineering*, 127(8), 663-670. [doi:10.1061/(ASCE)0733-9429(2001)127:8(663)]